Pre-compensation of Nonlinear Distortion of a Silicon Microring Modulator Using Back-calculation

Peng Wang, John C. Cartledge, Wai-Yip Chan
Department of Elcectrical and Computer Engineering, Queen's University
Kingston, Canada
peng.wang@queensu.ca

***Abstract*—A pre-compensation scheme for nonlinear distortion of a silicon microring modulator using back-calculation of the modulator model is proposed. The bit error ratio performance shows significant improvement with back-calculation for a 28 Gbaud PAM-4 signal transmitted over 15 km single mode fiber.**

I. Introduction

Silicon photonics is being widely investigated due to the potential for integration and the compatibility with CMOS technology [1]. Compared with silicon Mach-Zehnder modulators, silicon microring modulators (MRMs) have smaller chip size, lower power consumption, and enhanced modulation efficiency [2]. The modulation bandwidth is limited due to the resonance [3] and the modulation dynamics are nonlinear due to the Lorentzian transfer function, the nonlinear electro-optic effect, and the electrical nonlinearity of the reverse biased PN junction [4], [5]. Previously, a Volterra nonlinear equalizer has been used to post-compensate for the nonlinear modulation dynamics of an MRM [6]. In this paper, we propose a pre-compensation scheme for the nonlinear modulation dynamics by back-calculating the input drive signal based on governing rate equations and a defined modulator output intensity. The pre-compensated 28 Gbaud PAM-4 signal meets the hard decision forward error correction (FEC) coding threshold of 4.6×10^{-3} after transmission over 15 km single mode fiber (SMF).

II. Simulation Model

A silicon ring modulator consists of a bus waveguide and a closely placed micro-ring, as is shown in Fig. 1(a). When driven by an electrical signal, the refractive index of the PN junction changes accordingly, resulting in modulation of both the phase and intensity of the light circulating in the ring. The wavelength dependence of the resonance properties of an MRM under various DC bias voltages is shown in Fig. 1(b). Changing the bias voltage from 0 V to -3 V, shifts the wavelength of the resonance point by 68 pm, resulting in a sensitivity of 22.7 pm/V. Assuming the working wavelength of the laser coincides with the red line in Fig. 1(b) and the drive voltage swings between 0 V and -3 V, the shift of the transfer function induces intensity modulation.

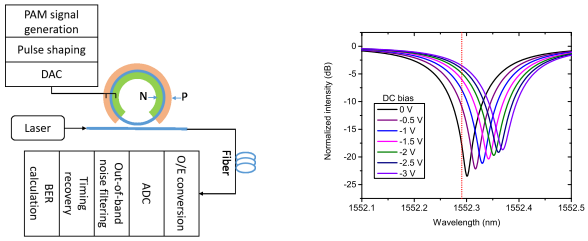

(a) (b)

Fig. 1: (a) Schematic diagram of intensity modulated ring modulator. (b) Ring resonance shift at different bias voltage.

According to coupling mode theory, the dynamic modulation of an MRM can be modelled by the following rate equations [7]:

$$\frac{d\phi(t)}{dt} = \left[-j\omega_r(t) - \frac{1}{\tau_a(t)} - \frac{1}{\tau_l}\right]\phi(t) + j\sqrt{\frac{2}{\tau_l}}E_{in} \quad (1)$$

$$E_{out} = E_{in} + j\sqrt{\frac{2}{\tau_l}}\phi(t) \quad (2)$$

where E_{in} and E_{out} are the complex-valued fields of the input and output signals, respectively, $\phi(t)$ is the optical signal circulating in the ring, $\omega_r(t)$ is the angular resonance frequency, $\tau_a(t)$ is the decay time due to free carrier absorption and intrinsic loss in the ring, and τ_l is the decay time constant due to coupling loss to the bus waveguide. $\omega_r(t)$ and $\tau_a(t)$ both depend on the applied electrical signal $V(t)$. By solving (1) and (2), the optical output signal of the modulator can be obtained. Importantly, the intensity and phase of a modulated optical signal are determined by $V(t)$.

The pre-compensation is based on predistorting the input drive signal by back-calculation of the rate equations to achieve a specified optical intensity at the output of the modulator. The accompanying optical phase modulation is then determined by the back-calculated $V(t)$. It has a direct impact on the distortion of a propagating signal and transmission performance due to fiber dispersion. Since the modulator output intensity $|E_{out}|^2$ is a function of $\omega_r(t)$ and $\tau_a(t)$, which are functions of the drive signal $V(t)$, the back-calculated drive signal can be determined for a desired output intensity. The predistorted drive signal compensates for the nonlinear modulation dynamics and produces a specified output optical intensity.

978-1-7281-1647-1/19/$31.00 ©2019 IEEE

III. Results and Discussion

The electrical signal used to drive the ring modulator is a 28 Gbaud PAM-4 signal. A 2^{18} de Bruijn bit sequence is mapped into four levels to form the PAM-4 symbols, which is then applied to a raised-cosine pulse shaping filter with a roll-off factor of 1. The drive signal has a peak-to-peak value of 3 V and a DC bias of -1.5 V. The CW wavelength of the laser is 1552.291 nm which corresponds to the red line in Fig. 1(b). At the receiver, the optical signal is first converted to electrical domain through square law detection of a photodiode with a 5th order Bessel response. The detected signal is applied to an ADC (2 samples/symbol), and filtered to remove out-of-band noise. Timing recovery is performed, following by symbol-to-bit demapping and bit error counting.

In order to pre-compensate for the nonlinear modulation dynamics, the desired optical intensity at the output of the modulator is defined as an offset raised cosine pulse with a roll-off factor of 1, which is taken as the input of the back-calculation model. The offset is set to ensure that the intensity is non-negative. The eye diagram of the back-calculated drive signal is shown in Fig. 2(a). Fig. 2(b) indicates this predistorted drive signal has frequency content over a broad range. Applying this drive signal to the ring modulator, an ideal optical intensity eye pattern is generated in Fig. 2(c).

In practice, the back-calculated drive signal is generated by a DAC. In the previous calculations, the limitations on the bandwidth and resolution of the DAC are not considered. In order to study this effect, an 8-bit DAC is implemented with the ideal back-calculated drive signal truncated to a bandwidth of 28 GHz. The DAC sampling rate is set to be 56 GSa/s to meet the Nyquist sampling criterion. The resultant optical intensity is shown in Fig. 2(d). Compared with the ideal case in Fig. 2(c), the eye opening is slightly degraded as shown in Fig. 2(d).

Fig. 3 presents the BER performance with and without back-calculation for a back-to-back system configuration and fiber transmission over 15 km. Back-calculation provides a small

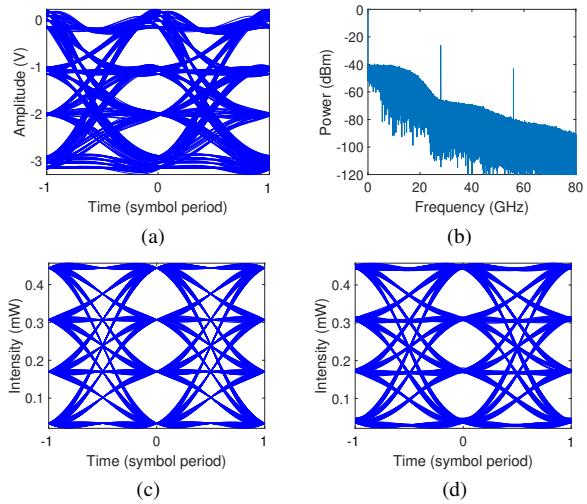

Fig. 2: Ideally back-calculated drive signal (a) eye diagram, (b) frequency spectrum. Intensity eye diagram at the output of the modulator with drive signal generated by (c) an ideal DAC, (d) a practical DAC with a bandwidth of 28 GHz and resolution of 8 bits.

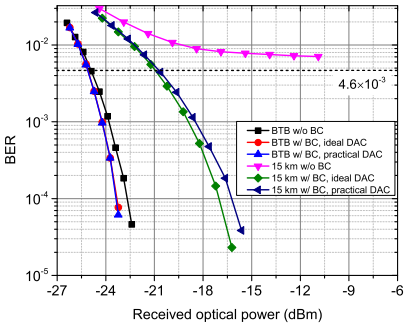

Fig. 3: Pre-FEC BER versus received optical power without back-calculation, with back-calculation and ideal DAC, with back-calculation and practical DAC for a back-to-back configuration and 15 km fiber transmission, respectively. BC: back-calculation.

improvement over the non-compensated curve for the back-to-back configuration. After transmission over 15 km SMF, non-compensated scheme exhibits a BER floor at 7×10^{-3}, while the back-calculation scheme meets the FEC BER threshold of 4.6×10^{-3} at a received optical power of -21 dBm. The dramatic improvement in transmission performance with the back-calculated drive signal is due to the stronger tolerance to fiber dispersion after compensation of nonlinear distortion. The implementation for the practical DAC has a small effect on the BER performance with back-calculation.

In conclusion, we have proposed a pre-compensation scheme for nonlinear distortion of a silicon MRM using back-calculation. The back-calculated PAM-4 signal exhibits improved BER performance after transmission of 15 km SMF. The impact of using a practical DAC in generating the drive signal is small, indicating the feasibility of ring modulator nonlinear pre-compensation.

Acknowledgement

The authors would like to thank Zhao Wang of McMaster University for his help with the modelling of MRMs.

References

[1] D. Thomson, A. Zilkie, J. E. Bowers, T. Komljenovic, G. T. Reed, L. Vivien, D. Marris-Morini, E. Cassan, L. Virot, J.-M. Fédéli, *et al.*, "Roadmap on silicon photonics," *Journal of Optics*, vol. 18, no. 7, p. 073003, 2016.

[2] L. Chrostowski and M. Hochberg, *Silicon photonics design: from devices to systems*. Cambridge University Press, 2015.

[3] Z. Wang, Y. Gao, A. S. Kashi, J. C. Cartledge, and A. P. Knights, "Silicon microring modulator for dispersion uncompensated transmission applications," *Journal of Lightwave Technology*, vol. 34, no. 16, pp. 3675–3681, 2016.

[4] A. M. Gutierrez, A. Brimont, J. Herrera, M. Aamer, D. J. Thomson, F. Y. Gardes, G. T. Reed, J.-M. Fedeli, and P. Sanchis, "Analytical model for calculating the nonlinear distortion in silicon-based electro-optic mach–zehnder modulators," *Journal of Lightwave Technology*, vol. 31, no. 23, pp. 3603–3613, 2013.

[5] S. Yu and T. Chu, "Electrical nonlinearity in silicon modulators based on reversed pn junctions," *Photonics Research*, vol. 5, no. 2, pp. 124–128, 2017.

[6] Y. Gao, Z. Wang, J. C. Cartledge, S. S.-H. Yam, and A. P. Knights, "56 Gb/s single-carrier 16-QAM and 32-QAM subcarrier modulation using a silicon micro-ring resonator," in *2017 Optical Fiber Communications Conference and Exhibition (OFC)*, pp. 1–3, IEEE, 2017.

[7] L. Zhang, Y. Li, J.-Y. Yang, M. Song, R. G. Beausoleil, and A. E. Willner, "Silicon-based microring resonator modulators for intensity modulation," *IEEE Journal of Selected Topics in Quantum Electronics*, vol. 16, no. 1, pp. 149–158, 2010.